Intestinal adenomas from $Apc^{Min/+}$; $Blm^{Cin/+}$ mice were evaluated for loss of heterozygosity (LOH) at the *Apc* locus, a feature typical of $Apc^{Min/+}$ adenomas (*24, 25*). Five adenomas from $Apc^{Min/+}$;$Blm^{+/+}$ mice and 20 adenomas from $Apc^{Min/+}$; $Blm^{Cin/+}$ mice were analyzed (Fig. 2C). The mean ratio of the Apc^+ to the Apc^{Min} allele in tumors from $Apc^{Min/+}$; $Blm^{Cin/+}$ mice was not different from that in tumors from $Apc^{Min/+}$;$Blm^{+/+}$ mice. Each was consistent with published values (*24, 25*), demonstrating loss of the WT *Apc* allele in all tumors from *Blm* heterozygous mice.

We next investigated the mutational mechanisms responsible for loss of the normal *Apc* allele in the intestinal tumors by LOH analysis. *Apc* maps to chromosome 18 and is located on the genetic map at 15.0 centimorgans (*26*). We used quantitative polymerase chain reaction (PCR) with simple sequence length polymorphism markers (*19*) for three loci to examine allelic loss on chromosome 18 in our set of 25 tumors (Fig. 2C). Tumors in $Apc^{Min/+}$;$Blm^{+/+}$ mice and 18 of 20 tumors in $Apc^{Min/+}$; $Blm^{Cin/+}$ mice were characterized by LOH of *Apc* and all markers proximal and distal to *Apc* on chromosome 18 (Fig. 2C). Two tumors from $Apc^{Min/+}$;$Blm^{Cin/+}$ mice, of which one is shown, remained heterozygous at the proximal marker *D18Mit19* (Fig. 2C). These results indicate that *Apc* loss in $Apc^{Min/+}$ tumors with two WT *Blm* alleles is characterized by LOH of chromosome 18 but that in some $Blm^{Cin/+}$ tumors, loss of the normal *Apc* allele occurs by somatic recombination.

To test whether the tumors from $Apc^{Min/+}$; $Blm^{Cin/+}$ mice retained the WT *Blm* allele, we performed a quantitative PCR-based assay on 14 tumors. The ratio of the WT to the targeted allele in each tumor sample from $Apc^{Min/+}$; $Blm^{Cin/+}$ mice was not significantly different from that in adjacent normal tissue (Fig. 2D). Western blots of 10 tumor lysates from $Apc^{Min/+}$;$Blm^{Cin/+}$ mice evaluated with antiserum to COOH-terminus of BLM confirmed that BLM expression had been retained (fig. S3A). Similarly, immunofluorescence of MLV-induced lymphomas from $Blm^{Cin/+}$ mice demonstrated nuclear BLM staining (fig. S3B). These results suggest that mutation of the remaining WT *Blm* allele was not required for tumor formation in either T cells or intestinal tissues.

Mutation of one allele of *Blm* has measurable consequences for the phenotype of murine somatic cells and for the tumor susceptibility of the mouse. Our data demonstrate that *Blm* haploinsufficiency is sufficient to affect tumor formation in susceptible mice, and probably alter genomic stability. These effects have not been described in other targeted *Blm* mice (*12, 13*). These data also suggest that *Blm* haploinsufficiency could promote tumor formation in tissues other than those studied here. Additionally, although

none of the tumors in $Apc^{Min/+}$;$Blm^{Cin/+}$ mice were invasive at the 4-month end point of our experiments, it is possible that these tumors would progress to malignancy if given more time. Our results are also important for human populations: About 1 in 100 Ashkenazi Jews carry one mutant allele of *BLM* (*25, 26*). An accompanying paper by Gruber *et al.* (*27*) demonstrates that carriers of BLM^{Ash} have a more than twofold increase in the occurrence of colorectal cancer. Together, these studies suggest that *Blm*/*BLM* mutation is an important modifier of intestinal cancer predisposition and that individuals carrying one mutant allele of *BLM* may have one of the noteworthy clinical hallmarks of BS—namely, increased cancer predisposition.

References and Notes
1. J. German, *Medicine* **72**, 393 (1993).
2. J. Groden, J. German, *Hum. Genet.* **90**, 360 (1992).
3. J. Groden, Y. Nakamura, J. German, *Proc. Natl. Acad. Sci. U.S.A.* **87**, 4315 (1990).
4. N. A. Ellis *et al.*, *Cell* **83**, 655 (1995).
5. N. A. Ellis, M. Proytcheva, M. M. Sanz, T.-Z. Ye, J. German, *Am. J. Hum. Genet.* **65**, 1368 (1999).
6. A. Bahr, F. De Graeve, C. Kedinger, B. Chatton, *Oncogene* **17**, 2565 (1998).
7. J. K. Karow, A. Constantinou, J. L. Li, S. C. West, I. D. Hickson, *Proc. Natl. Acad. Sci. U.S.A.* **97**, 6504 (2000).
8. H. Sun, J. K. Karow, I. D. Hickson, N. Maizels, *J. Biol. Chem.* **273**, 27587 (1998).
9. G. Langland *et al.*, *Cancer Res.* **62**, 2766 (2002).
10. L. Shahrabani-Gargir, *Genet. Test.* **2**, 293 (1998).
11. L. Li, C. Eng, R. J. Densnick, J. German, N. A. Ellis, *Mol. Genet. Metab.* **64**, 286 (1998).
12. N. Chester, F. Kuo, C. Kozak, C. D. O'Hara, P. Leder, *Genes Dev.* **12**, 3382 (1998).
13. G. Luo *et al.*, *Nature Genet.* **26**, 424 (2000).
14. J. Groden, unpublished data.
15. J. German, N. A. Ellis, M. Proytcheva, *Clin. Genet.* **49**, 223 (1996).
16. M. P. Rosin, J. German, *Hum. Genet.* **71**, 187 (1985).
17. M. M. Sanz, J. German, unpublished data.
18. R. H. Martin, A. Rademaker, J. German, *Am. J. Hum. Genet.* **55**, 1242 (1994).
19. Materials and methods are available as supporting material on *Science* Online.
20. A. M. Lowy *et al.*, *Gastroenterology* **121**, 435 (2001).
21. A. R. Moser, H. C. Pitot, W. F. Dove, *Science* **247**, 322 (1990).
22. L. K. Su *et al.*, *Science* **256**, 668 (1992).
23. C57BL/6J-Apc^{Min+} male mice (from the Jackson Laboratory) were mated to $Blm^{Cin/+}$ female mice (backcrossed to 129/SvEv to the N_3 generation) to obtain progeny that were $Apc^{Min/+}$;$Blm^{+/+}$ or $Apc^{Min/+}$; $Blm^{Cin/+}$. Mice were genotyped for the Apc^{Min} mutation, and tumors were quantified as previously described by C. L. Wilson *et al.* [*Proc. Natl. Acad. Sci. U.S.A.* **94**, 1402 (1997)].
24. D. B. Levy *et al.*, *Cancer Res.* **54**, 5953 (1994).
25. C. Luongo, A. R. Moser, S. Gledhill, W. F. Dove, *Cancer Res.* **54**, 5947 (1994).
26. C. Luongo *et al.*, *Genomics* **15**, 3 (1993).
27. S. S. Gruber *et al.*, *Science* **297**, 2013 (2002).
28. We thank the University of Cincinnati Comparative Pathology and Gene Targeting Facilities, J. Mante, and T. Reichling for assistance. Supported by the Ohio Cancer Research Foundation; the National Cancer Institute Mouse Models of Human Cancer Consortium (grant CA84291); the Center for Environmental Genetics at the University of Cincinnati (grant ES06096); the National Institutes of Health [grants CA63507 (J.G.) and CA88460 (K.H.G.)]; and the Howard Hughes Medical Institute.

Cleavage of *Scarecrow-like* mRNA Targets Directed by a Class of *Arabidopsis* miRNA

Cesar Llave, Zhixin Xie, Kristin D. Kasschau, James C. Carrington*

Micro-RNAs (miRNAs) are regulatory molecules that mediate effects by interacting with messenger RNA (mRNA) targets. Here we show that *Arabidopsis thaliana* miRNA 39 (also known as miR171), a 21-ribonucleotide species that accumulates predominantly in inflorescence tissues, is produced from an intergenic region in chromosome III and functionally interacts with mRNA targets encoding several members of the *Scarecrow-like* (*SCL*) family of putative transcription factors. miRNA 39 is complementary to an internal region of three *SCL* mRNAs. The interaction results in specific cleavage of target mRNA within the region of complementarity, indicating that this class of miRNA functions like small interfering RNA associated with RNA silencing to guide sequence-specific cleavage in a developmentally controlled manner.

Micro-RNAs in eukaryotes are ~21- to 22-ribonucleotide RNAs that arise from short stem-loop precursors through the activity of the double-stranded ribonuclease Dicer (*1–6*). The miRNAs from *lin-4* and *let-7* genes are involved in translational control through interaction with 3′-proximal sequences in tar-

get mRNAs in *Caenorhabditis elegans* (*7–11*). However, the range of functions for other miRNAs in plants, animals, and microorganisms has yet to be determined.

Arabidopsis contains numerous small RNAs, many of which resemble miRNAs identified in animals (*12, 13*). Several of

these, including miRNA 39, have sequence identity or complementarity to mRNAs for protein-coding genes. miRNA 39 accumulates predominantly in inflorescence tissue and was predicted to arise from a precursor gene in an intergenic region (IGR) in chromosome III (*12, 13*). The miRNA 39 sequence and predicted stem-loop structure of the putative precursor are conserved in the genome of rice (*Oryza sativa*) (*13*). We detected miRNA 39–like species in *Arabidopsis*, rice, and *Nicotiana benthamiana* by blot assay (Fig. 1A). The *Arabidopsis*, rice, and *N. benthamiana* miRNA 39 accumulated to relatively high levels in inflorescence and flower tissues (Fig. 1A, lanes 3, 6, and 8) and to lower or nondetectable levels in leaf and stem tissue (Fig. 1A, lanes 1, 2, 4, 5, and 7).

The miRNA 39 sequence in *Arabidopsis* is perfectly complementary to an internal sequence in mRNAs of three members [*SCL6-II* (locus At2g45160), *SCL6-III* (locus At3g60630), and *SCL6-IV* (locus At4g00150)] of the *Scarecrow-like* family of putative transcription factors (*12, 13*). Four *SCL* genes in rice have complementarity to miRNA 39 (*13*). Members of the *SCL* family control a wide range of developmental processes, including radial patterning in roots and hormone signaling (*14–17*). No other small RNAs related to sequences from the 3′-proximal regions of *SCL6-III* or *SCL6-IV* genes were detected in *Arabidopsis* leaf, stem, or inflorescence tissues by blot assay [fig. S1A (*18*)], indicating that miRNA 39 was not part of a larger small interfering RNA (siRNA) population resulting from general RNA silencing triggered against broader segments of the *SCL* mRNAs. Blot assays indicated that *SCL6-III* and *SCL6-IV* genes were expressed in leaf, stem, and inflorescence tissues (Fig. 1B), although *SCL6-III* and *SCL6-IV* mRNAs were most abundant in inflorescence tissue (Fig. 1B, lanes 5, 6, 13, and 14). In addition to full-length mRNAs [designated SCL6-III(a) and SCL6-IV(a) RNAs], shorter RNAs [SCL6-III(b) and SCL6-IV(b)] of ~1.4 and ~1.3 kilobases (kb), respectively, were detected with a 3′-proximal probe in extracts from inflorescence tissue but not in extracts from stems or leaves (Fig. 1B, lanes 5, 6, 13, and 14).

The 5′ ends of SCL6-III(b) and SCL6-IV(b) RNAs were mapped by 5′ RACE (rapid amplification of cDNA ends) to positions corresponding to the middle of the respective sequences complementary to miRNA 39 (Fig. 1B). The 5′-RACE reac-
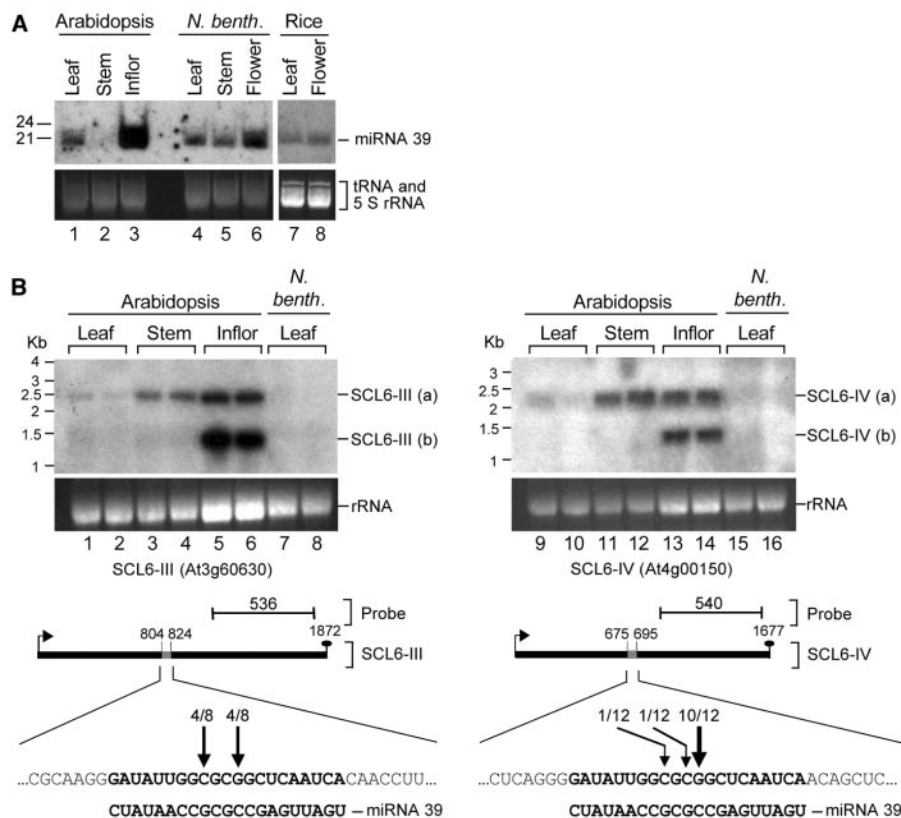
Center for Gene Research and Biotechnology, and Department of Botany and Plant Pathology, Oregon State University, Corvallis, OR 97331, USA.

*To whom correspondence should be addressed. E-mail: carrington@orst.edu

Fig. 1. Expression of *SCL* genes and miRNA 39. (**A**) RNA blot analysis of miRNA 39 from *Arabidopsis* and *N. benthamiana* leaf, stem, and inflorescence/flower tissue and from rice (*O. sativa*) leaf and flower tissue. (**B**) RNA blot analysis of *SCL6-III* (left) and *SCL6-IV* (right) mRNAs. Normalized (10 μg per lane) RNA samples from *Arabidopsis* leaf, stem, and inflorescence tissue were analyzed in duplicate. The proportion of total RNA represented by the large cytoplasmic ribosomal RNA (rRNA) (shown in ethidium bromide–stained gels) differs between tissue types in *Arabidopsis*, which accounts for the more abundant rRNA in the inflorescence samples. The protein-coding regions (nucleotide numbering begins at the start codon) and the locations of the sequences complementary to miRNA 39 are shown in the expanded diagrams. *SCL6-III*– and *SCL6-IV*–specific probes detected both full-length mRNA [SCL6-III(a) and SCL6-IV(a)] and shorter RNA [SCL6-III(b) and SCL6-IV(b)] in inflorescence tissue. The positions corresponding to the 5′ ends of the SCL6-III(b) and SCL6-IV(b) RNAs determined by 5′ RACE, and the number of 5′-RACE clones corresponding to each site, are indicated by arrows.

tions involved ligation of an adapter to the 5′ end without enzymatic pretreatment, suggesting that both RNAs contained a ligation-competent 5′ monophosphate rather than a conventional 5′ cap. These results are consistent with a model in which the SCL6-III(b) and SCL6-IV(b) RNAs arise by sequence-specific cleavage of the full-length mRNAs at a site directed by miRNA 39. In effect, miRNA 39 may function like a single siRNA (*19*), produced in trans from a miRNA 39 precursor gene, that guides cleavage of target *SCL* mRNAs. As siRNA-guided cleavage of silencing targets occurs at positions centered in the middle of siRNA-target RNA duplexes (*20*), both siRNA-guided and miRNA 39–guided cleavage might occur by a common mechanism within a sequence-specific nucleolytic complex termed RISC (RNA-induced silencing complex) (*21, 22*). This model predicts that accumulation of SCL6-III(b)

and SCL6-IV(b) RNAs will correlate with accumulation of miRNA 39, which is consistent with the tissue-specific distribution patterns of miRNA 39 and SCL6-III(b) and SCL6-IV(b) RNAs (*12*) (Fig. 1, A and B).

We tested the hypothesis that miRNA 39 functions to direct cleavage of *SCL* mRNAs with an *Agrobacterium*-mediated delivery (Agro-inoculation) system to coexpress miRNA 39 and SCL6-IV target mRNA in *N. benthamiana* leaf tissue. We reasoned that a miRNA 39 precursor could be produced through transcription of the miRNA 39–containing IGR, either with an endogenous miRNA 39 promoter or with a 35*S* promoter, followed by Dicer-like processing (*13*) of the precursor in *N. benthamiana*. Three constructs with the complete miRNA 39–containing IGR, or empty vector as a control, were coexpressed with the *SCL6-IV* construct (*35S:SCL6-IV*). Two of the constructs (*35S:IGR-mi39* and *35S:AS-IGR-mi39*) contained

Fig. 2. Cleavage of *SCL6-IV* mRNA is directed by miRNA 39. (**A**) Constructs containing the miRNA 39–containing IGR and the *SCL6-IV* coding sequence were co–Agro-inoculated in *N. benthamiana* leaves, and normalized extracts were tested for miRNA 39 by RNA blot assay 2 and 3 days postinoculation (d p.i.). (**B**) Analysis of SCL6-IV (a) and (b) RNA forms in normalized extracts from co–Agro-inoculated tissue by RNA blot assay with probes corresponding to 3′ (top) or 5′ (bottom) regions of the *SCL6-IV* coding sequence. The amount of SCL6-IV(b) RNA, expressed as a percentage of total SCL6-IV RNA [(a) + (b)], is indicated for each sample. The blots were stripped and reanalyzed with a cytoplasmic rRNA probe. The position of sequence complementary to miRNA 39 is indicated in gray in the diagram. The size of the SCL6-IV(b) RNA (~1.3 kb) corresponds to the 3′-proximal SCL6-IV sequence (~1.0 kb) plus the 3′-untranslated sequence (~0.3 kb). At, *A. thaliana*; Nb, *N. benthamiana*.
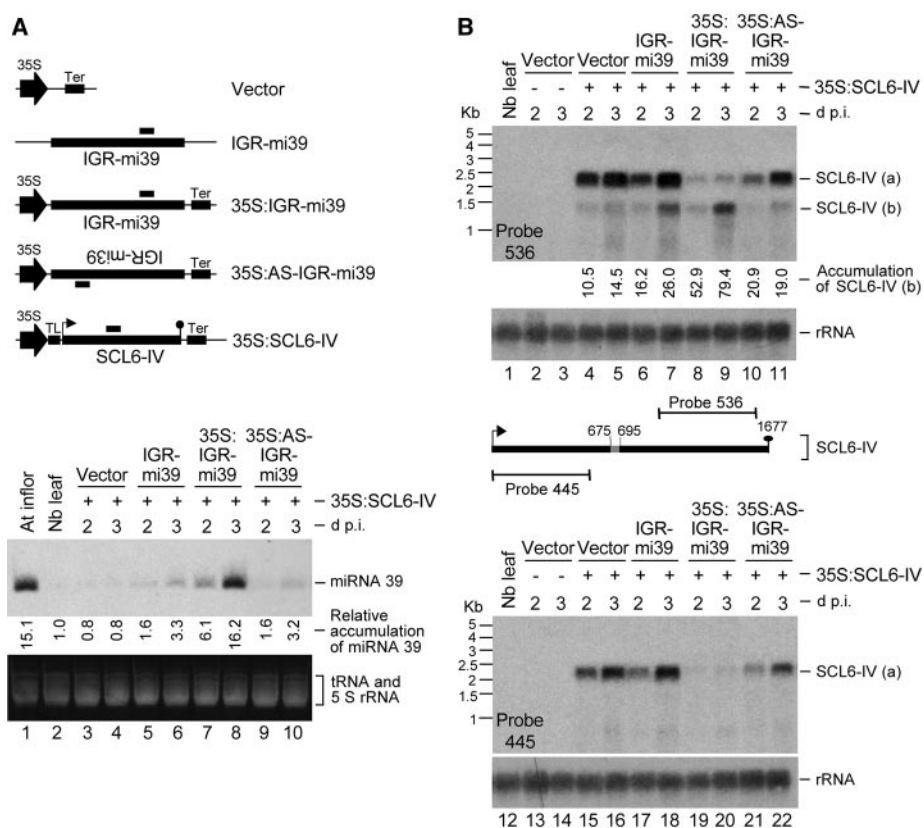
a 35*S* promoter for production of synthetic IGR transcripts of sense (relative to miRNA 39) or antisense orientation, respectively, and one (*IGR-mi39*) contained the IGR sequence without a 35*S* promoter (Fig. 2A). A basal level of endogenous miRNA 39 was detected in nontreated leaves (Fig. 2A, lane 2) and in leaves that were co–Agro-inoculated with *35S:SCL6-IV* and the empty vector (lanes 3 and 4). High levels of miRNA 39 were produced after co–Agro-inoculation with the sense-oriented *35S:IGR-mi39* construct (Fig. 2A, lanes 7 and 8), indicating that the synthetic RNA transcript was recognized accurately by a Dicer-like enzyme (*13*). Data showing that miRNA 39 accumulation in these experiments was not the result of generalized RNA silencing of *SCL* genes or the 35*S* promoter–driven constructs are provided in the SOM text (*18*). Only low levels of miRNA 39 above background were detected in tissues expressing the antisense-oriented *35S:AS-IGR-mi39* (Fig. 2A, lanes 9 and 10) or IGR-mi39 constructs (lanes 5 and 6). The low levels of miRNA 39 directed by the *IGR-mi39* construct suggest that the IGR sequence contains relatively weak regulatory sequences for transcription of the miRNA 39 precursor gene, or that the miRNA 39 precursor gene is suppressed, in *N. benthamiana* leaf tissue.

Coexpression of *35S:IGR-mi39* and *35S:SCL6-IV* resulted in internal cleavage of the *SCL6-IV* mRNA (Fig. 2B, top, lanes 8 and 9).
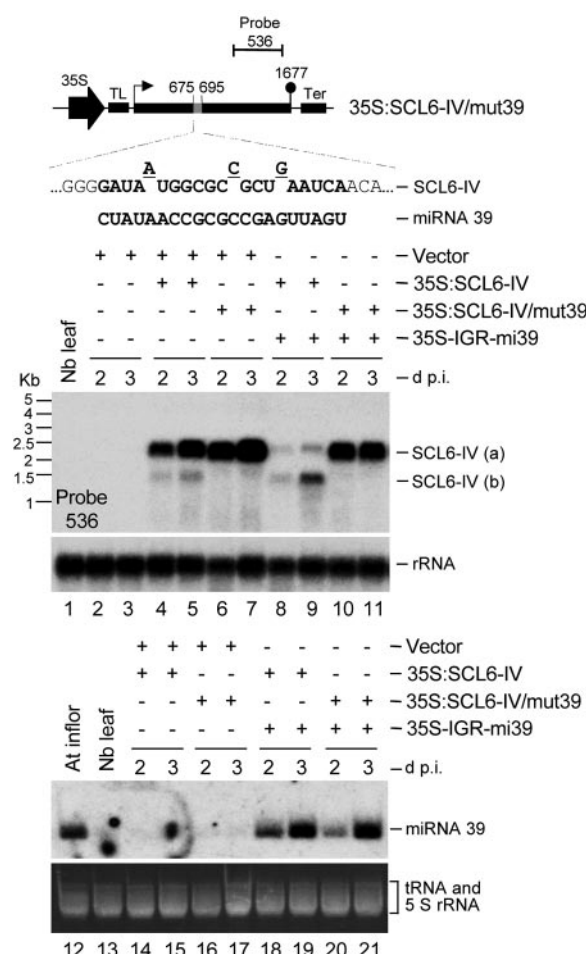
Fig. 3. Cleavage of *SCL6-IV* mRNA requires sequence complementarity to miRNA 39. Mutations (underlined) were introduced into the *35S:SCL6-IV/mut39* construct, and wild-type and mutant constructs were co–Agro-inoculated with the *35S:IGR-mi39* construct in *N. benthamiana*. SCL6-IV RNA forms (top) and miRNA 39 (bottom) in extracts at 2 and 3 d p.i. were analyzed by blot assay. The SCL6-IV RNA blot was hybridized with a probe corresponding to the 3′ end of the *SCL6-IV* coding region and then reanalyzed with a cytoplasmic rRNA probe.

About 53 and 79% of the *SCL6-IV*–related RNA detected 2 and 3 days postinfiltration, respectively, corresponded to the SCL6-IV(b) RNA product. Relatively small proportions of *SCL6-IV* mRNA were cleaved after coexpression with empty vector (Fig. 2B, top, lanes 4 and 5), *IGR-mi39* (lanes 6 and 7), and *35S:AS-IGR-mi39* constructs (lanes 10 and 11), which can be explained by the basal or low levels of miRNA 39 in these samples. No cleavage products were detected with the SCL6-IV 5′-end probe (Fig. 2B), suggesting that the 5′ fragment was less stable than the 3′ fragment [SCL6-IV(b)]. Identical results were obtained when the *SCL6-III* mRNA was used as a target in coexpression assays (*23*).

To determine whether cleavage of *SCL6-IV* mRNA depends on perfect complementarity with miRNA 39, we introduced three mismatches into the sequence complementary to miRNA 39 in *SCL6-IV* RNA (construct *35S:SCL6-IV/mut39*) (Fig. 3). Whereas the wild-type *SCL6-IV* mRNA was cleaved efficiently in the presence of the miRNA 39–producing *35S:IGR-mi39* construct (Fig. 3, lanes 8, 9, 18, and 19), the *SCL6-IV/mut39* mRNA was completely resistant to cleavage (lanes 10, 11, 20, and 21). Furthermore, the low level of cleavage of *SCL6-IV* mRNA in the presence of the empty vector construct was inhibited by the mutations (Fig. 3, lanes 4 to 7), confirming that this activity was due to low levels of endogenous miRNA 39 in *N. benthamiana* tissue.

The finding of miRNA-directed cleavage of several *SCL* mRNA targets in *Arabidopsis* indicates that there are at least two functional classes of miRNAs. Members of the small temporal RNA (stRNA)–like class, including *C. elegans lin-4* and *let-7* miRNAs, down-regulate translation of target mRNAs but do not direct RNA target degradation or site-specific cleavage (*7, 8, 10, 11*). The stRNA class members do not interact with perfect complementarity to their natural targets, which may explain why they do not exhibit siRNA-like activity (*24*). In contrast, members of a class represented by *Arabidopsis* miRNA 39 interact with perfect complementarity and appear to mimic siRNA function to guide cleavage. We propose that miRNA 39 incorporates into a RISC-like complex identical or similar to the RISC complex that mediates target cleavage during RNA silencing (*21, 22*). Support for this concept also comes from the finding that engineered miRNA-target combinations with perfect complementarity result in target RNA cleavage (*25, 26*). Finally, miRNA 39–guided cleavage of mRNAs has several possible consequences, including developmentally coordinated inactivation of *SCL* mRNAs. Internal cleavage might also generate RNA products with novel characteristics or coding potential for truncated SCL proteins. Given the number of miRNAs that were recently discovered in eukaryotes (*4–6, 12, 13, 27, 28*), additional members will likely be added to each class.

References and Notes

1. E. Bernstein, A. A. Caudy, S. M. Hammond, G. J. Hannon, *Nature* **409**, 363 (2001).
2. G. Hutvágner et al., *Science* **293**, 834 (2001).
3. R. F. Ketting et al., *Genes Dev.* **15**, 2654 (2001).
4. M. Lagos-Quintana, R. Rauhut, W. Lendeckel, T. Tuschl, *Science* **294**, 853 (2001).
5. N. C. Lau, E. P. Lim, E. G. Weinstein, D. P. Bartel, *Science* **294**, 858 (2001).
6. R. C. Lee, V. Ambros, *Science* **294**, 862 (2001).
7. R. C. Lee, R. L. Feinbaum, V. Ambros, *Cell* **75**, 843 (1993).
8. B. Wightman, I. Ha, G. Ruvkun, *Cell* **75**, 855 (1993).
9. E. G. Moss, R. C. Lee, V. Ambros, *Cell* **88**, 637 (1997).
10. B. J. Reinhart et al., *Nature* **403**, 901 (2000).
11. F. J. Slack et al., *Mol. Cell* **5**, 659 (2000).
12. C. Llave, K. D. Kasschau, M. A. Rector, J. C. Carrington, *Plant Cell* **14**, 1605 (2002).
13. B. J. Reinhart, E. G. Weinstein, M. W. Rhoades, B. Bartel, D. P. Bartel, *Genes Dev.* **16**, 1616 (2002).
14. L. DiLaurenzio et al., *Cell* **86**, 423 (1996).
15. A. L. Silverstone, C. N. Ciampaglio, T. Sun, *Plant Cell* **10**, 155 (1998).
16. C. Bolle, C. Koncz, N. H. Chua, *Genes Dev.* **14**, 1269 (2000).
17. Y. Helariutta et al., *Cell* **101**, 555 (2000).
18. Materials and methods are available as supporting material on *Science* Online.
19. A. J. Hamilton, D. C. Baulcombe, *Science* **286**, 950 (1999).
20. S. M. Elbashir, W. Lendeckel, T. Tuschl, *Genes Dev.* **15**, 188 (2001).
21. S. M. Hammond, E. Bernstein, D. Beach, G. J. Hannon, *Nature* **404**, 293 (2000).
22. S. M. Hammond, S. Boettcher, A. A. Caudy, R. Kobayashi, G. J. Hannon, *Science* **293**, 1146 (2001).
23. C. Llave, J. C. Carrington, unpublished data.
24. G. Ruvkun, *Science* **294**, 797 (2001).
25. M. T. McManus, C. P. Petersen, B. B. Haines, J. Chen, P. A. Sharp, *RNA* **8**, 842 (2002).
26. G. Hutvágner, P. D. Zamore, *Science* **297**, 2056 (2002); published online 1 August 2002 (10.1126/science.1073827).
27. Z. Mourelatos et al., *Genes Dev.* **16**, 720 (2002).
28. E. C. Lai, *Nature Genet.* **30**, 363 (2002).
29. We thank L. Johansen, M. Rector, and B. Shaffer for valuable comments and technical support. We are also grateful to J. Valkonen and J. Kreuze for helpful suggestions on 5′-RACE procedures and D. Olszyk for providing rice tissue. C.L. was the recipient of a postdoctoral fellowship from the Ministerio de Educación y Cultura (Spain). This work was supported by grant MCB-0209836 from the National Science Foundation, grants AI27832 and AI43288 from NIH, and grant NRI 2002-35319-11560 from the U.S. Department of Agriculture.

A microRNA in a Multiple-Turnover RNAi Enzyme Complex

György Hutvágner and Phillip D. Zamore*

In animals, the double-stranded RNA-specific endonuclease Dicer produces two classes of functionally distinct, tiny RNAs: microRNAs (miRNAs) and small interfering RNAs (siRNAs). miRNAs regulate mRNA translation, whereas siRNAs direct RNA destruction via the RNA interference (RNAi) pathway. Here we show that, in human cell extracts, the miRNA *let-7* naturally enters the RNAi pathway, which suggests that only the degree of complementarity between a miRNA and its RNA target determines its function. Human *let-7* is a component of a previously identified, miRNA-containing ribonucleoprotein particle, which we show is an RNAi enzyme complex. Each *let-7*–containing complex directs multiple rounds of RNA cleavage, which explains the remarkable efficiency of the RNAi pathway in human cells.

Two types of 21- to 23-nucleotide (nt) RNAs are produced by the multidomain ribonuclease (RNase) III enzyme Dicer: small interfering RNAs (siRNAs) from long double-stranded RNA (*1, 2*) and microRNAs (miRNAs) from ~70-nt hairpin precursor RNAs whose expression is often developmentally regulated (*3–8*). siRNAs direct the cleavage of complementary mRNA targets, a process known as RNA inter-

ference (RNAi) (*9*). Target RNA cleavage is catalyzed by the RNA-induced silencing complex (RISC), which acts as an siRNA-directed endonuclease, cleaving the target RNA across from the center of the complementary siRNA strand (*10, 11*). Assembly of the RISC is adenosine triphosphate (ATP) dependent and precedes target recognition (*10, 12*). Unlike siRNAs, miRNAs are single stranded and pair with target mRNAs that contain sequences only partially complementary to the miRNA and repress mRNA translation without altering mRNA stability (*13–19*). Although at least 135 miRNAs have been identified collectively from *Caenorhabditis elegans*, *Drosophila melanogaster*, and humans, none is fully complementary to

Department of Biochemistry and Molecular Pharmacology, University of Massachusetts Medical School, Lazare Research Building, Room 825, 364 Plantation Street, Worcester, MA 01605, USA.

*To whom correspondence should be addressed. E-mail: phillip.zamore@umassmed.edu